



## Research paper

## Polymer-based spherical activated carbon as catalytic support for hydrodechlorination reactions

Macarena Munoz<sup>a,\*</sup>, Veronika Kolb<sup>b</sup>, Ana Lamolda<sup>a</sup>, Zahara M. de Pedro<sup>a</sup>, Antje Modrow<sup>c</sup>, Bastian J.M. Etzold<sup>d,\*</sup>, Juan J. Rodriguez<sup>a</sup>, Jose A. Casas<sup>a</sup>

<sup>a</sup> Sección Departamental de Ingeniería Química, Universidad Autónoma de Madrid, 28049, Madrid, Spain

<sup>b</sup> Lehrstuhl für Chemische Reaktionstechnik, Friedrich-Alexander-Universität Erlangen-Nürnberg, 91058, Erlangen, Germany

<sup>c</sup> Blücher GmbH, 14727, Premitz, Germany

<sup>d</sup> Ernst-Berl-Institut für Technische und Makromolekulare Chemie, Technische Universität Darmstadt, 64287, Darmstadt, Germany

## ARTICLE INFO

## Article history:

Received 27 March 2017

Received in revised form 6 June 2017

Accepted 1 July 2017

Available online 3 July 2017

## Keywords:

PBSAC  
Catalytic hydrodechlorination  
Palladium  
4-chlorophenol

## ABSTRACT

In this work, polymer-based spherical activated carbon (PBSAC) ( $d_p = 500 \mu\text{m}$ ) has been used as support to synthesize several Pd/PBSAC (1% wt.) catalysts. These catalysts have been tested in the hydrodechlorination (HDC) of 4-chlorophenol (4-CP) in aqueous phase under ambient-like conditions ( $30^\circ\text{C}$ , 1 atm) at  $[4\text{-CP}]_0 = 3.9 \text{ mmol L}^{-1}$ ;  $[\text{catalyst}]_0 = 1 \text{ g L}^{-1}$  and  $50 \text{ N mL H}_2 \text{ min}^{-1}$ . A sequential calcination ( $200^\circ\text{C}$ , air atmosphere) – reduction ( $80^\circ\text{C}$ ,  $\text{H}_2$  atmosphere) treatment was required to obtain active HDC catalysts with a convenient proportion of zero-valent and electrodefficient Pd species. This catalyst allowed to achieve complete conversion of 4-CP in 90 min reaction time, giving rise to phenol as main reaction product. An expanded kinetic model accounting for both consecutive reaction and sorption processes was used to successfully fit the experimental data. The values obtained for the effective rate constant of 4-CP disappearance ( $3.26\text{--}10.88 \times 10^{-4} \text{ s}^{-1}$ ) and apparent activation energy ( $31.6 \text{ kJ mol}^{-1}$ ) were close to the previously reported for powdered supported Pd catalysts. Remarkably, the catalyst showed a high stability in long-term continuous application (100 h on stream).

© 2017 Elsevier B.V. All rights reserved.

## 1. Introduction

Organochlorinated compounds are among the most distributed pollutants in water [1–4]. The presence of these xenobiotic contaminants in the environment is of increasing concern given their high toxicity, carcinogenic character and long-term persistence in the ecosystems. Their ecological effects and impact on public health have promoted increasingly stringent regulations, being a priority in Europe and the US. Among the potential solutions investigated for the treatment of those pollutants, catalytic hydrodechlorination (HDC) has been claimed as an effective and environmentally-friendly technology, becoming a burgeoning topic in environmental catalysis [3]. HDC allows a fast conversion of a wide range of chlorinated contaminants into less harmful products under ambient-like operating conditions. Apart from the clear environmental benefit, the application of HDC to treat highly concentrated effluents

could be also interesting from an economic point of view since the resulting dechlorinated by-products could be recovered.

A number of catalysts have been tested in HDC, but those based on Pd have received major attention due to their higher activity, selectivity and stability compared to other metals such as Rh, Pt or Ni [5–7]. Meanwhile, activated carbon (AC) has been identified as one of the most suitable supports for HDC catalysts due to its high resistance towards the HCl generated upon reaction. On the other hand, the high adsorption capacity of AC has demonstrated to play a key role on the kinetics of the process. For instance, HDC rate constants were around six times higher with Pd/AC than those obtained with Pd/ $\text{Al}_2\text{O}_3$  (1% wt.;  $d_p = 24 \mu\text{m}$ ) commercial catalysts at similar loading and metal particle size [8]. Additional advantages of AC as catalytic support are its high surface area, the tunability of porosity and surface chemistry and the low interaction with catalytically active species [9].

Conventional ACs, derived from natural sources like coal or wood, are usually fine powders or low-stable granules, difficult to handle and recover. Their ash contents have also to be considered. In this context, the use of ACs produced from synthetic polymer precursors as starting materials represents a promising alternative given their high and homogeneous quality, their well-

\* Corresponding authors.

E-mail addresses: [macarena.munoz@uam.es](mailto:macarena.munoz@uam.es) (M. Munoz), [etzold@tc1.tu-darmstadt.de](mailto:etzold@tc1.tu-darmstadt.de) (B.J.M. Etzold).

defined pore texture and their very low or practically negligible ash content. Furthermore, polymers can be provided in different shapes, being the sphere one of the most interesting for wastewater treatment applications due to its excellent dynamic behavior and high resistance to abrasion [10,11]. Furthermore, polymers can be provided in different shapes, being the sphere one of the most interesting for wastewater treatment applications due to its excellent dynamic behavior and high resistance to abrasion [10,11]. Polymer-based spherical activated carbons (PBSACs) have been so far mainly used in sorption processes [12–14] but have also proved to be interesting supports in different catalytic applications [15–19]. PBSAC-supported palladium catalysts have been successfully tested in the liquid-phase (ethanol) hydrogenation of cinnamic acid in a recent contribution [20] but its use for the HDC of organochlorinated pollutants in water has not been reported so far.

Recently, we demonstrated that deducing true kinetic constants from catalytic HDC experiments with high surface area supports is only possible if adsorption is considered in the kinetic model [8]. This allows to predict reaction progress and selectivity successfully. Therefore, the application of novel carbon supports should always include a kinetic modelling comprising both sorption and HDC processes to allow the comparison of different catalysts regardless their sorption capacity as well as the estimation of their performance at technical scale.

In the current work, the application of PBSAC-supported palladium catalysts has been investigated in the HDC of 4-chlorophenol (4-CP). The preparation of the catalyst was accomplished by oxidizing the PBSAC support with sulfuric acid in order to break its hydrophobic character and introduce oxygen groups favouring Pd anchorage [20]. Pd was then incorporated by ion-exchange [20]. To investigate the effect of the oxidation state of Pd species on HDC the subsequent thermal treatment of the resulting Pd/PBSAC catalyst was varied. Its activity has been tested under different operating conditions and an expanded kinetic model accounting for sorption and reaction has been accordingly developed to fit the experimental data. Finally, the stability of Pd/PBSAC has been assessed in a long-term continuous experiment.

## 2. Materials and methods

### 2.1. Materials

The PBSAC support (particle size 500 µm), based on polystyrene-divinylbenzene as precursor, was provided by Blücher GmbH, Germany. Palladium (II) chloride (99%), phenol (99%), cyclohexanone (99%) and cyclohexanol (99%) were supplied by Sigma-Aldrich. Sulfuric acid (96%) and hydrochloric acid (37% wt.) were purchased from Panreac and 4-chlorophenol (99%) from Fluka. All the reagents were used as received without further purification.

### 2.2. Preparation and characterization of Pd/PBSAC catalysts

Prior to metal impregnation, the PBSAC was oxidized for 2 h at 90 °C with 10 mL of sulfuric acid (50% vol.) per gram of carbon. A reflux condenser prevented evaporation. The solid was separated by filtration, washed until neutral filtrate and dried overnight at 60 °C in a vacuum oven.

Immobilization of Pd on the functionalized-PBSAC was carried out by ion-adsorption from an aqueous solution of  $\text{PdCl}_2$  and HCl ( $\text{pH} = 1$ ). The ratio of precursor solution to PBSAC was  $10 \text{ mL g}^{-1}$ , to adjust the palladium loading of the catalyst to 1% wt nominal. After the addition of PBSAC, the suspension was slowly stirred at room temperature for 24 h and then filtered and washed with 200 mL of HCl solution of equal pH as the impregnation one. The obtained solid was then dried at 60 °C in a vacuum oven overnight.

The resulting Pd/PBSAC catalyst was submitted to different thermal treatments. In the first set, the catalyst was reduced with hydrogen ( $50 \text{ N mL min}^{-1}$ ) at 80 °C for 2 h. In the second series, a calcination step at 200 °C in air atmosphere for 4 h was performed prior to reduction. The catalysts were denoted as PBSAC-r and PBSAC-cr, where -r and -cr represent the kind of thermal treatment applied in their preparation (r: reduction (80 °C); cr: calcination (200 °C) followed by reduction (80 °C)).

The porous texture of the PBSAC-based catalysts was characterized from nitrogen adsorption-desorption at –196 °C using a Micromeritics Tristar II 3020 apparatus. The samples were previously outgassed overnight at 150 °C to a residual pressure of  $<10^{-3}$  Torr. Data evaluation was performed with the software Tristar II version V1.03 using the quenched solid density functional theory (QSDFT) for slit pores. The specific surface area was calculated by the BET equation and the micropore volume was estimated by Dubinin-Radushkevich method. The difference between the  $\text{N}_2$  adsorbed volume at a relative pressure of  $P/P^0 = 0.95$  and the micropore volume was taken as mesopore volume. The palladium content of the catalysts was determined by total reflection X-ray fluorescence (TXRF), using a TXRF spectrometer 8030c. Surface palladium species were analysed by X-ray photoelectron spectroscopy (XPS) with a Thermo Scientific K-Alpha apparatus equipped with a  $\text{K}\alpha$  X-ray excitation source, 1486.68 eV. The software “XPS-Peak” was used for spectrograms deconvolution. Thermogravimetric analyses (TG) were performed with a TGA/SDTA851e (Mettler Toledo) thermogravimetric analyser under air atmosphere at a heating rate of  $10^\circ\text{C min}^{-1}$ , from 30 to 900 °C.

### 2.3. Typical reaction procedure

HDC experiments were performed batch-wise in a magnetically stirred glass slurry-type reactor (500 mL) equipped with temperature control. The reaction took place during 3 h under vigorous stirring (1000 rpm) and continuous feeding of  $\text{H}_2$  ( $50 \text{ N mL min}^{-1}$ ). The starting concentration of the target pollutant and the reaction volume were fixed at  $3.9 \text{ mmol L}^{-1}$  and 350 mL, respectively. Unless otherwise indicated, a catalyst concentration of  $1 \text{ g L}^{-1}$  was used whereas the temperature was tested within the 20–50 °C range. Each run was carried out by triplicate being the standard deviation less than 5% in all cases. The long-term continuous experiment (100 h) was performed using the same reactor but including a PTFE blade stirrer instead of the magnetic one. The volume was fixed at 350 mL and the initial concentration of 4-CP at 1.6 mM. The hydrogen flow was maintained at  $50 \text{ N mL min}^{-1}$  while the liquid stream was fed at  $1 \text{ mL min}^{-1}$ , which corresponds to  $3.65 \text{ kg}_{\text{cat}} \text{ h mol}^{-1}$  space-time.

The progress of the HDC experiments was followed by periodically withdrawing samples from the reactor. 4-CP, phenol (Ph), cyclohexanone (C-one) and cyclohexanol (C-ol) were analysed by a gas chromatograph with a 25 m length x 0.32 mm i.d. capillary column (CP-FFAP CB, Varian) coupled to a flame ionization detector (GC 3900, Varian).

Equilibrium adsorption tests were also carried out under the same operating conditions as the HDC runs but in the absence of hydrogen. Solutions of 4-CP and the main HDC product, Ph, were prepared at concentrations from 1.5 to  $8 \text{ mmol L}^{-1}$ . The Langmuir equation was used to fit the equilibrium data (Eq. (1)).

$$q_i = \frac{K_{\text{SORP}_i} \cdot q_{mi} \cdot C_i}{1 + K_{\text{SORP}_i} \cdot C_i} \quad (1)$$

$i = 4\text{-CP, Ph}$ .

where  $q_i$  is the amount of the  $i$  species onto the catalyst at equilibrium ( $\text{mmol gcat}^{-1}$ );  $C_i$  is the equilibrium concentration of that species in the liquid phase ( $\text{mmol L}^{-1}$ );  $K_{\text{SORP}_i}$  is the Langmuir

**Table 1**

Characterization of the catalysts.

Material	BET surface area ( $\text{m}^2 \text{ g}^{-1}$ )	Pore volume ( $\text{cm}^3 \text{ g}^{-1}$ )	Micropore volume ( $\text{cm}^3 \text{ g}^{-1}$ )	Mesopore volume ( $\text{cm}^3 \text{ g}^{-1}$ )	Pd (% wt.)	$\text{Pd}^0/\text{Pd}^{n+}$
PBSAC	1755	1.07	0.78	0.29	–	–
Pd/PBSAC-r	1714	1.03	0.76	0.27	1.03	Only $\text{Pd}^0$
Pd/PBSAC-cr	1717	1.04	0.77	0.27	1.03	0.38

constant ( $\text{L mmol}^{-1}$ ) and  $q_{\text{mi}}$  is the maximum adsorption capacity ( $\text{mmol gcat}^{-1}$ ).

### 3. Results and discussion

#### 3.1. Catalysts characterization

**Table 1** summarizes the characterization of the prepared catalysts. PBSAC is an essentially microporous solid with a high BET surface of  $1755 \text{ m}^2 \text{ g}^{-1}$ , containing micropores and mesopores within a broad distribution (see Fig. S1 of the Supplementary Material for the  $\text{N}_2$  sorption isotherms). After oxidation of the carbon with  $\text{H}_2\text{SO}_4$  a complete Pd deposition through ion-adsorption was achieved for the target loading of 1% wt. On the other hand, the surface area of the resulting catalysts was similar to that of the pristine support. These results are consistent with the reported by Klefer et al. [20] with the same carbon material and different oxidation agents ( $\text{H}_2\text{SO}_4$  and  $\text{HNO}_3$ ). In that work, although both treatments allowed successful impregnation of Pd in the range of 1–10% wt., the oxidation with  $\text{HNO}_3$  led to appreciable area losses (up to 15%) opposite to  $\text{H}_2\text{SO}_4$  treatment which did not alter the surface area of the starting carbon.

The HDC reaction can be influenced by the oxidation state of the Pd species on the catalyst [21–24]. To learn on that, different calcination and reduction treatments were applied to prepare the final catalysts. First, TG analyses in air atmosphere were carried out, demonstrating that both PBSAC and Pd/PBSAC are thermally stable up to  $530^\circ\text{C}$  (see Fig. S2 of the Supplementary Material for the TG curves), which is much higher than the calcination temperatures in the current work. As can be seen in **Table 1** and **Fig. 1**, the reduction of Pd/PBSAC in  $\text{H}_2$  atmosphere led to the formation of  $\text{Pd}^0$  as the only species whereas the calcination in air prior to reduction gave rise to both  $\text{Pd}^0$  and  $\text{Pd}^{n+}$  species. Taking into account that the concentration of Pd on the outermost surface (XPS) was significantly lower than the bulk one (TXRF) ( $\text{Pd}_{\text{surface}}/\text{Pd}_{\text{bulk}} = 0.3$ ), it can be concluded that the catalyst preparation method favoured the location of Pd in the internal porosity of the support. On the other hand, the catalysts were also characterized by TEM to learn on the dispersion and particle size of Pd after the different thermal treatments. Both Pd/PBSAC-r and Pd/PBSAC-cr catalysts showed a homogeneous dispersion of Pd onto the carbon surface and no significant differences were observed among them on this respect (See Fig. S3 of the Supplementary Material for STEM images).

#### 3.2. Activity of the Pd/PBSAC catalysts: influence of the preparation conditions

**Fig. 2** shows the evolution of 4-CP and the reaction products upon HDC with Pd/PBSAC-r and Pd/PBSAC-cr at  $30^\circ\text{C}$ . The thermal treatment used in the synthesis of those materials was crucial regarding their catalytic activity. Pd/PBSAC-r, submitted only to reduction ( $\text{H}_2$ ,  $80^\circ\text{C}$ ) showed a negligible activity, being the disappearance of 4-CP due to adsorption. Neither chloride nor Ph or any further hydrogenation product were detected so that HDC is not taking place. On the opposite, the catalyst undergoing a calcination step (air,  $200^\circ\text{C}$ ) prior to the reduction one (Pd/PBSAC-cr) yielded complete dechlorination at the end of the reaction (3 h). The final concentrations of Ph and C-one are far from covering

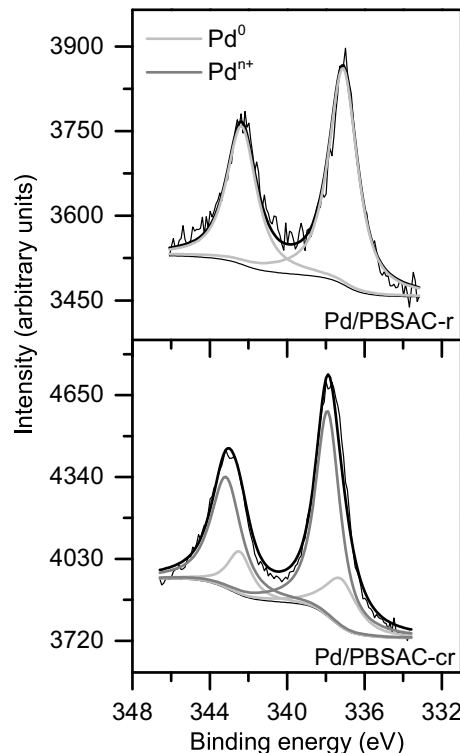


**Fig. 1.** Deconvolution of the Pd 3d core-level spectra of Pd/PBSAC-r and Pd/PBSAC-cr.

the carbon balance and thus, adsorption of any of those species must be quite important. It is then clear that the presence of both palladium species ( $\text{Pd}^{n+}$  and  $\text{Pd}^0$ ) is needed for HDC activity, in agreement with previous works in the literature [21–24]. Gomez-Sainero et al. [21] found that a  $\text{Pd}^0/\text{Pd}^{n+}$  ratio close to 1 was optimum for the liquid-phase hydrodechlorination of  $\text{CCl}_4$ . According to these results, further experiments of the current work will use only the Pd/PBSAC-cr catalyst.

The high surface area and the nature of the PBSAC support are consistent with the abovementioned occurrence of adsorption. The disappearance of 4-CP can be attributed essentially to HDC as the concentration of  $\text{Cl}^-$  at the end of the experiment (3 h) represented more than 95% of the initial chlorine in 4-CP. Ph (the primary product from HDC) and/or its further hydrogenation by-products are partially adsorbed onto the catalyst. The evolution of reaction products indicates that the HDC proceeds according to a consecutive reaction pathway where 4-CP reacts with hydrogen to produce Ph, which is further converted into C-one [8,23–25].

A parallel set of experiments was carried out under the same operating conditions as the HDC ones but in the absence of  $\text{H}_2$  to discriminate the effect of adsorption and reaction on the kinetics at different temperatures. As representative example, **Fig. 3** shows the results obtained in both the adsorption and HDC runs at  $30^\circ\text{C}$  (see Fig. S3 of the Supplementary Material for data at other temperatures). As observed, there was no difference in the disappearance of 4-CP operating with or without  $\text{H}_2$  until the adsorption equilibrium was reached ( $\sim 20$  min). It should be also noted that

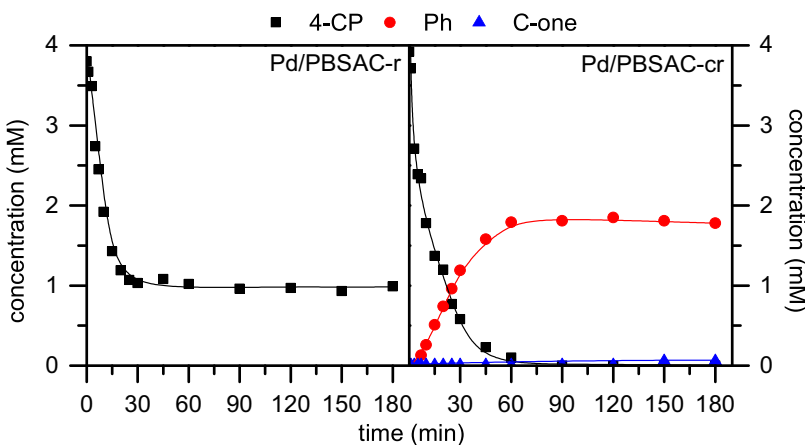
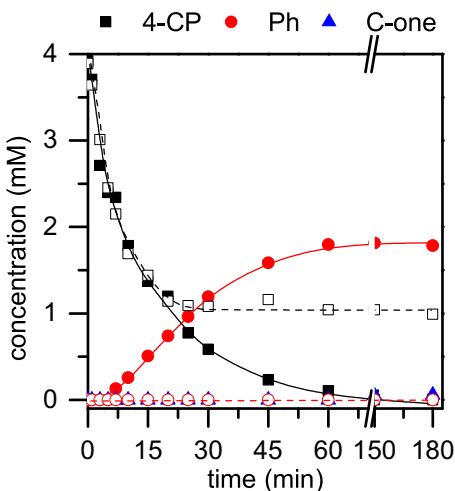


Fig. 2. HDC of 4-CP with Pd/PBSAC-r and Pd/PBSAC-cr catalysts at 30 °C.

Fig. 3. Evolution of 4-CP and reaction by-products upon treatment with the Pd/PBSAC-cr catalyst in the presence (solid symbols) and absence (open symbols) of  $\text{H}_2$ .

with  $\text{H}_2$  the HDC product Ph started to be detected after 7 min reaction time, when 4-CP disappearance was already around 40%. That shifting was less pronounced as temperature increased. From the species identified in the liquid phase, the carbon balance was far from closure. Adsorption of both 4-CP and Ph onto the catalyst played an important role, being the prevailing contribution in the earlier stages of the process. It can be then concluded that the sorption behaviour of those species is clearly different taking into account that 4-CP is completely hydrodechlorinated along the

**Table 2**  
Langmuir parameters for 4-CP and Ph adsorption onto Pd/PBSAC at 30 °C.

	$K_{\text{SORP}}$ ( $\text{L mmol}^{-1}$ )	$q_m$ ( $\text{mmol g}_{\text{cat}}^{-1}$ )	$R^2$
4-CP	13.5	3.03	0.99
Ph	1.06	3.33	0.99

reaction ( $[\text{Cl}^-]_{\text{aqueousphase}} = 3.8 \text{ mM}$ ) but the amount of free Ph in solution was higher than the free 4-CP at equilibrium in the adsorption experiment.

Additionally, the single adsorption of the target pollutant (4-CP) and the main HDC product (Ph) onto Pd/PBSAC-cr without  $\text{H}_2$  feeding were investigated. Fig. 4 depicts the adsorption isotherms at 30 °C. The values of the Langmuir equilibrium constant ( $K_{\text{SORP}}$ ) and the maximum uptake ( $q_m$ ) are collected in Table 2. They are comparable with the reported by other authors for the adsorption of 4-CP and Ph onto different activated carbons [8,26–28]. The equilibrium constant for 4-CP was significantly higher (up to 10 times) than the obtained for Ph whereas quite similar values were obtained for  $q_m$ . On the other hand, those  $q_m$  values were remarkably higher than the reported in a previous contribution [8] with commercial Pd on activated carbon catalysts. This fact can be explained by the significantly higher surface area of PBSAC ( $>1700 \text{ m}^2 \text{ g}^{-1}$ ) compared to those catalysts ( $700\text{--}900 \text{ m}^2 \text{ g}^{-1}$ ).

### 3.3. Kinetic analysis

#### 3.3.1. Mass transfer considerations

Possible mass-transfer limitations during the HDC reaction were evaluated experimentally by varying the stirring velocity, catalyst concentration and particle size. The stirring velocity showed no

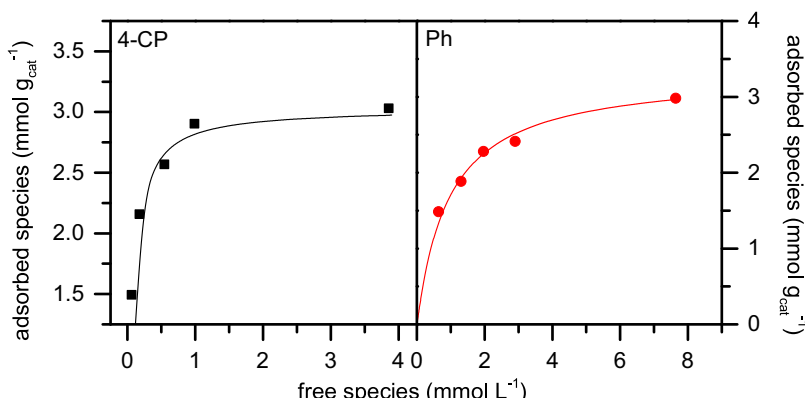


Fig. 4. Experimental data (symbols) and Langmuir fits (solid lines) for the adsorption equilibrium of 4-CP and Ph onto Pd/PBSAC-cr at 30 °C.

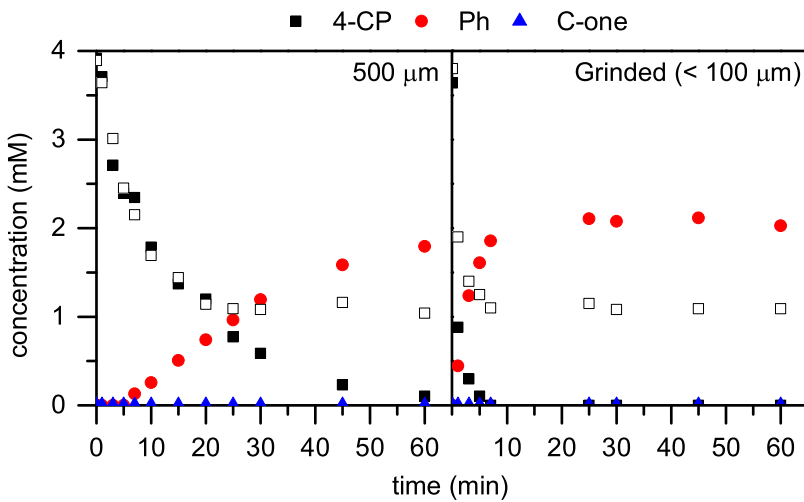


Fig. 5. Time-course of 4-CP, Ph and C-one upon adsorption (open symbols) and HDC (solid symbols) with Pd/PBSAC-cr at 30 °C.

effect on the rate of 4-CP disappearance within the 800–1200 rpm range (see Fig. S4 of the Supplementary Material for experimental data) and the reaction rate increased linearly with the catalyst concentration (see Fig. S5 of the Supplementary Material for details). Thus, external mass transfer and gas-liquid transfer limitations can be discarded.

To evaluate the possible existence of internal mass transfer limitation with the catalyst up to 500 μm particle size, it was grinded to obtain a fine powder (80–100 μm) and HDC as well as adsorption experiments were carried out. The results are collected in Fig. 5 and show a pronounced increase of the rate of 4-CP disappearance with the smaller particles, both in presence and absence of H<sub>2</sub>. Further experiments were carried out at smaller catalyst size (63–80 and 30–63 μm) (data not shown) and the results were quite similar to the obtained at 80–100 μm. Thus it can be said that 100 μm is about the critical size where the transition from chemical reaction to pore diffusion-controlled kinetics occurs. Therefore, the adsorption as well as the overall reaction proceed under internal mass-transfer control with the 500 μm catalyst.

### 3.3.2. Model set-up

The proposed kinetic model is based on the reaction pathway depicted in Scheme 1. Pseudo-first order kinetics was adopted for each individual reaction step and the contribution of adsorption was considered. As has been previously demonstrated, adsorption of the main compounds involved in the reaction plays a key role in HDC. Thus, an expanded kinetic model, which accounts for both sorption and HDC, has been developed [8]. Effective kinetic constants were deduced at this step, including the effect of pore diffusion limitations. It is assumed that adsorption takes place essentially onto the PBSAC support [27]. The parallel sorption processes are incorporated according to the Langmuir assumptions: i) total number of free and occupied sorption sites is maintained constant; ii) adsorption follows apparent first-order kinetics respect to the catalyst free sites and the solution concentration of adsorbate; and iii) desorption kinetics is of first order respect to the adsorbed species concentration. The net production rates of the compounds involved in the overall reaction can be expressed by Eqs. (2)–(6):

$$\frac{dC_{4CP}}{dt} = -k_{ADS-4CP} \cdot C_{4CP} \cdot (L_{max} - C_{4CPADS} - C_{PhADS}) + \frac{k_{ADS-4CP} \cdot C_{4CPADS}}{K_{SORP-4CP}} \quad (2)$$

$$\begin{aligned} \frac{dC_{4CPADS}}{dt} &= k_{ADS-4CP} \cdot C_{4CP} \cdot (L_{max} - C_{4CPADS} - C_{PhADS}) \\ &- \frac{k_{ADS-4CP} \cdot C_{4CPADS}}{K_{SORP-4CP}} - k_{HDC1} \cdot C_{4CPADS} \end{aligned} \quad (3)$$

$$\begin{aligned} \frac{dC_{Ph}}{dt} &= -k_{ADS-Ph} \cdot C_{Ph} \cdot (L_{max} - C_{4CPADS} - C_{PhADS}) \\ &+ \frac{k_{ADS-Ph} \cdot C_{PhADS}}{K_{SORP-Ph}} \end{aligned} \quad (4)$$

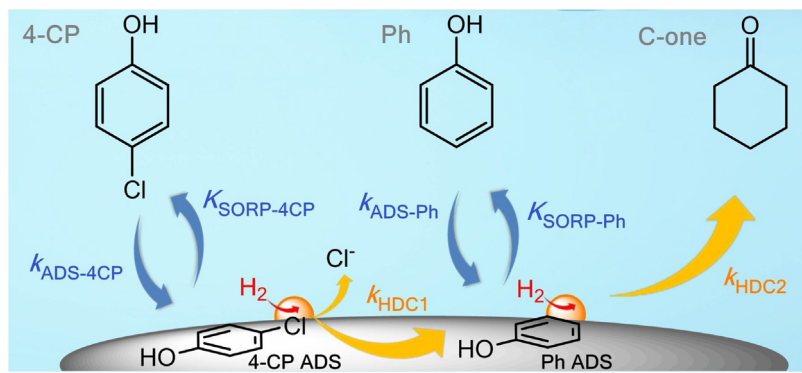
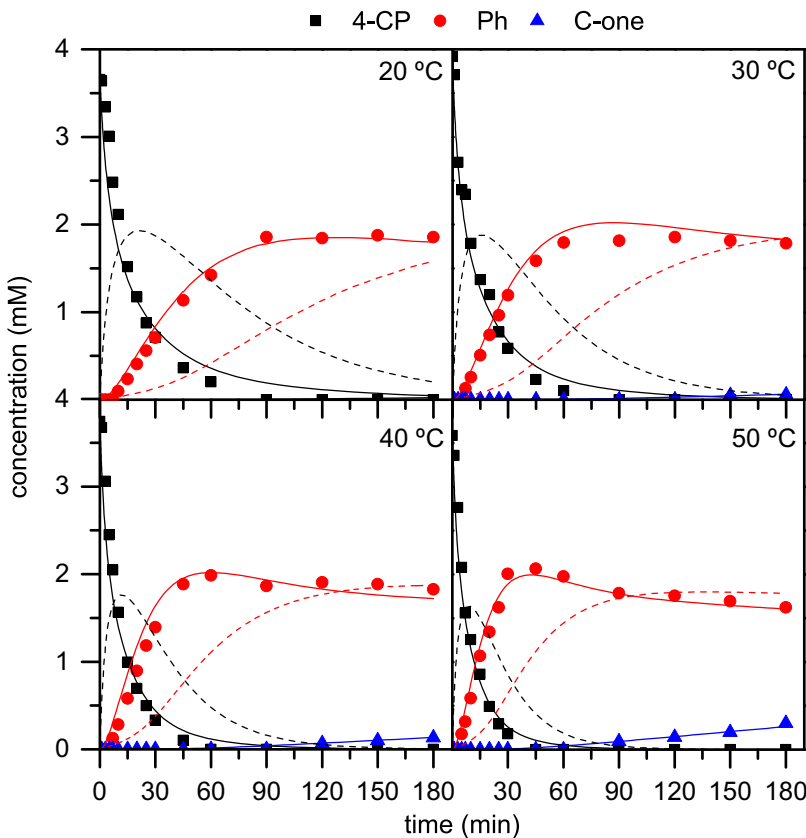
$$\begin{aligned} \frac{dC_{PhADS}}{dt} &= k_{ADS-4CP} \cdot C_{4CP} \cdot (L_{max} - C_{4CPADS} - C_{PhADS}) \\ &- \frac{k_{ADS-4CP} \cdot C_{4CPADS}}{K_{SORP-4CP}} + k_{HDC1} \cdot C_{4CPADS} - k_{HDC2} \cdot C_{PhADS} \end{aligned} \quad (5)$$

$$\frac{dC_{C-one}}{dt} = k_{HDC2} \cdot C_{PhADS} \quad (6)$$

where C<sub>4CP</sub>, C<sub>Ph</sub> and C<sub>C-one</sub> are the concentrations of 4-CP, Ph and C-one in solution (mmol L<sup>-1</sup>); C<sub>4CPADS</sub> and C<sub>PhADS</sub> are the concentrations of 4-CP and Ph adsorbed onto the PBSAC (mmol L<sup>-1</sup>); k<sub>HDC1</sub> and k<sub>HDC2</sub> are the apparent first order rate constants (s<sup>-1</sup>) for the HDC of 4-CP to Ph and the hydrogenation of Ph to C-one, respectively (Scheme 1); k<sub>ADS-4CP</sub> and k<sub>ADS-Ph</sub> are the adsorption rate constants (L mmol<sup>-1</sup> s<sup>-1</sup>) of 4-CP and Ph; K<sub>SORP-4CP</sub> and K<sub>SORP-Ph</sub> are the Langmuir adsorption equilibrium constants (L mmol<sup>-1</sup>) for 4-CP and Ph and L<sub>max</sub> represents the amount of free sites (mmol L<sup>-1</sup>) in the PBSAC calculated as q<sub>m4-CP</sub> · C<sub>Pd/PBSAC-cr</sub> · L<sub>max</sub> concentrations came from the parallel sorption experiments whereas rate (k<sub>HDC</sub> and k<sub>ADS</sub>) and equilibrium (K<sub>SORP</sub>) constants were fitting parameters for the HDC reaction.

### 3.3.3. Model evaluation

The expanded kinetic model was capable of describing accurately the experimental results obtained in the HDC of 4-CP with the Pd/PBSAC-cr catalyst within the range of temperature tested (20–50 °C) (Fig. 6). The values of the kinetic constants are collected in Table 3. Despite the observed pore diffusion limitations, the effective rate constants for the HDC of 4-CP are in the vicinity of those previously obtained in the literature with Pd catalysts [7]. As expected for Pd, 4-CP dechlorination rate constants were much higher (two orders of magnitude) than the obtained for the subsequent hydrogenation of Ph [7]. The values of apparent activation

**Scheme 1.** Scheme of the reaction pathway for the HDC of 4-CP with Pd/PBSAC-cr.**Fig. 6.** Evolution of 4-CP, Ph and C-one upon HDC with Pd/PBSAC-cr at different temperatures. Experimental (symbols) and model fit (solid lines: free species, dash lines: adsorbed species).**Table 3**

Values of the effective rate constants, apparent activation energies and sorption equilibrium constants for the HDC of 4-CP with Pd/PBSAC-cr at different temperatures.

T (°C)	$k_{\text{HDC}1} \times 10^4$ ( $\text{s}^{-1}$ )	$k_{\text{HDC}2} \times 10^6$ ( $\text{s}^{-1}$ )	$k_{\text{ADS}-4\text{CP}}$ ( $\text{L mmol}^{-1} \text{s}^{-1}$ )	$k_{\text{ADS}-\text{Ph}}$ ( $\text{L mmol}^{-1} \text{s}^{-1}$ )	$K_{\text{SORP}-4\text{CP}}$ ( $\text{L mmol}^{-1}$ )	$K_{\text{SORP}-\text{Ph}}$ ( $\text{L mmol}^{-1}$ )	$R^2$
20	3.26	2.85	0.64	0.98	13.48	1.07	0.99
30	5.01	5.41	0.79	1.17	13.18	0.98	0.99
40	7.47	9.87	0.95	1.39	12.90	0.90	0.99
50	10.88	17.3	1.14	1.62	12.65	0.83	0.99
Ea ( $\text{kJ mol}^{-1}$ )	31.6	47.4	15.0	13.3	—	—	0.99

energy ( $E_a$ ) for the different HDC reaction steps ranged from 10 to 50  $\text{kJ mol}^{-1}$ . These values are in good agreement with those quoted elsewhere [7,8,23,27].

The expanded kinetic model did not only allow describing successfully the evolution of the free species in the liquid phase but also predicting the progress of the adsorbed ones onto the PBSAC

support (Fig. 6). According to the proposed kinetic model, almost all free and adsorbed 4-CP was dechlorinated at the end of the experiment. This assumption was confirmed by the analysis of chloride ion in the liquid phase which accounted for more than 95% of the initial chlorine in 4-CP.

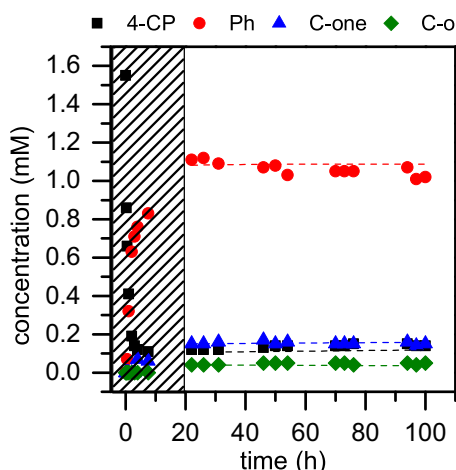


**Fig. 7.** Long-term performance of the Pd/PBSAC-cr catalyst upon HDC of 4-CP ( $[4\text{-CP}]_0 = 1.6 \text{ mM}$ ;  $T = 30^\circ\text{C}$ ;  $\tau = 3.65 \text{ kg}_{\text{cat}} \text{ h mol}^{-1}$ ).

### 3.4. Catalyst stability

The performance of the Pd/PBSAC-cr catalyst in a long-term continuous experiment is shown in Fig. 7. As observed, the catalyst exhibited a high stability not being detected any significant loss of activity upon the 100 h on stream once the steady-state was reached ( $\sim 20 \text{ h}$ ). Ph was the main reaction product whereas C-one and C-ol appeared at significantly lower concentrations. The presence of the latter can be related to the higher residence time in this experiment compared to the previous batch-wise runs, allowing hydrogenation of C-one. Although in the earlier stages the adsorption of the reaction species onto PBSAC impeded to close the carbon and chlorine balances, they were always matched in more than 90 and 95%, respectively, once the steady-state was achieved.

The catalyst was characterized by XPS at the end of the experiment to evaluate possible changes on the Pd species. A  $\text{Pd}^0/\text{Pd}^{n+}$  ratio of 1.07 was determined, which confirms the partial reduction of the catalyst under the operating conditions. The high stability of the catalyst along the reaction suggests that reduction takes place during its earlier stage prior to reach the steady state. The chlorine content of the used catalyst was negligible, demonstrating the resistance of Pd/PBSAC-cr to chloride poisoning, claimed as one of the main causes of catalyst deactivation in HDC [3,23].

These results are comparable to those reported for Pd on commercial activated carbon [29,30] and better than the obtained with inorganic supports such as pillared clays or alumina [23,30]. However, in the work of Diaz et al. [29] significantly higher space-times than in the current work were required (100 vs. 36  $\text{g}_{\text{Pd}} \text{ h mol}^{-1}$ ). Molina et al. [23] studied the HDC of 4-CP using Pd supported on powdered pillared clay under similar operating conditions ( $5.2 \text{ kg}_{\text{cat}} \text{ h mol}^{-1}$ ;  $25^\circ\text{C}$ ). A stable performance of the catalyst in terms of dechlorination was demonstrated but a decay of activity for further hydrogenation of Ph was observed, which was attributed to chloride poisoning. De Pedro et al. [30] also found a decrease on the activity of commercial Pd/ $\text{Al}_2\text{O}_3$  upon continuous HDC of 4-CP. The better performance of the AC-supported catalysts is associated with its high resistance to the chloride released upon HDC. Those authors suggested that AC interacts strongly with that species thus protecting the metallic active phase.

It is important to highlight that Pd/PBSAC-cr also showed a high mechanical strength and abrasion resistance due to its compact spherical shape [10], remaining the size and shape of the catalyst particles almost unchanged after the long-term experiment (see Fig. S7 of the Supplementary Material for light microscopic images of the fresh and used catalyst). This represents an outstanding

advantage regarding potential application compared to the finely powdered catalysts mostly reported so far in the literature [23,31].

### 4. Conclusions

PBSAC has proved to be a promising catalytic support for aqueous-phase HDC. The method followed in the preparation of the catalyst, comprising the oxidation of PBSAC in sulfuric acid, Pd deposition by ion-adsorption and gas-phase thermal treatment (calcination followed by reduction), allowed full and homogeneous immobilization of Pd on the support. The active phase included both  $\text{Pd}^0$  and  $\text{Pd}^{n+}$  species, crucial to obtain an active HDC catalyst. The experimental data were well described by an expanded kinetic model which considers the sequential adsorption and reaction steps. Despite the pore diffusion limitations observed, the values obtained for the HDC rate constants were similar to those previously reported in the literature for commercial Pd catalysts using other supports. In this sense, the Pd/PBSAC catalyst offers unprecedented advantages derived from its easy handling which facilitates separation and recovery. Furthermore, the possible loss of fine catalyst particles within the effluent, which is crucial in wastewater treatment, is greatly reduced. Strikingly, the catalyst maintained unchanged its HDC activity upon long-term application. In summary, the Pd/PBSAC catalyst has proved to be active, easily-recoverable and durable for the HDC reaction with 4-CP as model compound, although further research is needed with other chlorinated species and real wastewaters to learn more on its potential application.

### Acknowledgments

This research has been supported by the CM through the project S2013/MAE-2716 and by the Spanish MINECO through the project CTQ2013-4196-R. M. Munoz thanks the Spanish MINECO for a Juan de la Cierva-Incorporación postdoctoral contract (IJCI-2014-19427).

### Appendix A. Supplementary data

Supplementary data associated with this article can be found, in the online version, at <http://dx.doi.org/10.1016/j.apcatb.2017.07.001>.

### References

- [1] M.J. Gómez, S. Herrera, D. Solé, E. García-Calvo, A.R. Fernández-Alba, *Anal. Chem.* 83 (2011) 2638–2647.
- [2] Y. Persson, A. Shchukarev, L. Öberg, M. Tysklind, *Environ. Sci. Pollut. Res.* 15 (2008) 463–471.
- [3] M.A. Keane, *ChemCatChem* 3 (2011) 800–821.
- [4] P. Lampi, T. Vartiainen, J. Toumisto, A. Hesso, *Chemosphere* 20 (1990) 625–634.
- [5] F.J. Urbano, J.M. Marinas, *J. Mol. Catal. A: Chem.* 173 (2001) 329–345.
- [6] E.V. Golubina, E.S. Lokteva, S.A. Kachevsky, A.O. Turakulova, V.V. Lunin, *Stud. Surf. Sci. Catal.* 175 (2010) 293–296.
- [7] E. Díaz, J.A. Casas, A.F. Mohedano, L. Calvo, M.A. Gilarranz, J.J. Rodríguez, *Ind. Eng. Chem. Res.* 47 (2008) 3840–3846.
- [8] M. Munoz, M. Kaspareit, B.J.M. Etzold, *Chem. Eng. J.* 285 (2016) 228–235.
- [9] D. Comandella, S. Woszidlo, A. Georgi, F. Kopinke, K. Mackenzie, *Appl. Catal. B* 186 (2016) 204–211.
- [10] B. Böhringer, O. Guerra Gonzalez, I. Eckle, M. Müller, J. Giebelhausen, C. Schrage, S. Fichtner, *Chem. Ing. Tech.* 83 (2011) 53–60.
- [11] A.J. Romero-Anaya, M. Ouzzine, M.A. Lillo-Ródenas, A. Linares-Solano, *Carbon* 68 (2014) 296–307.
- [12] S. Yenisoy-Karakas, A. Aygün, M. Güneş, E. Tahtasakal, *Carbon* 42 (2004) 477–484.
- [13] Q. Wang, X. Liang, W. Qiao, C. Liu, X. Liu, L. Zhan, L. Ling, *Fuel Process. Technol.* 90 (2009) 381–387.
- [14] C. Schrage, A. Modrow, S. Fichtner, J. Giebelhausen, B. Böhringer, *Chem. Ing. Tech.* 86 (2014) 27–34.
- [15] S.B. de Oliveira, D.P. Barbosa, A.P. de Melo Monteiro, D. Rabelo, M.d.C. Rangel, *Catal. Today* 133–135 (2008) 92–98.

- [16] S. Fichtner, J. Hofmann, A. Möller, C. Schrage, J.M. Giebelhausen, B. Böhringer, R. Gläser, *J. Hazard. Mater.* 262 (2013) 789–795.
- [17] M. Ouzzine, A.J. Romero-Anaya, M.A. Lillo-Ródenas, A. Linares-Solano, *Carbon* 67 (2014) 104–118.
- [18] M.J. Schneider, M. Lijewski, R. Woelfel, M. Haumann, P. Wasserscheid, *Angew. Chem. Int. Ed.* 52 (2013) 6996–6999.
- [19] A. Weiß, M. Munoz, A. Haas, F. Rietzler, H.P. Steinrück, M. Haumann, P. Wasserscheid, B.J.M. Etzold, *ACS Catal.* 6 (2016) 2280–2286.
- [20] H. Klefer, M. Munoz, A. Modrow, B. Böhringer, P. Wasserscheid, B.J.M. Etzold, *Chem. Eng. Technol.* 39 (2016) 276–284.
- [21] L.M. Gomez-Sainero, X.L. Seoane, J.L.G. Fierro, A. Arcoya, *J. Catal.* 209 (2002) 279–288.
- [22] J.A. Baeza, L. Calvo, M.A. Gilarranz, A.F. Mohedano, J.A. Casas, J.J. Rodriguez, *J. Catal.* 293 (2012) 85–93.
- [23] C.B. Molina, A.H. Pizarro, J.A. Casas, J.J. Rodriguez, *Appl. Catal. B* 148–149 (2014) 330–338.
- [24] M. Munoz, Z.M. de Pedro, J.A. Casas, J.J. Rodriguez, *Appl. Catal. A* 488 (2014) 78–85.
- [25] T.T. Bovkun, Y. Sasson, J. Blum, *J. Mol. Catal. A: Chem.* 242 (2005) 68–73.
- [26] M. Streat, J.W. Patrick, M.J.C. Perez, *Water Res.* 29 (1995) 467–472.
- [27] Yu. Shindler, Yu. Matatov-Meytal, M. Sheintuch, *Ind. Eng. Chem. Res.* 40 (2001) 3301–3308.
- [28] Q. Liu, T. Zheng, P. Wang, J. Jiang, N. Li, *Chem. Eng. J.* 157 (2010) 348–356.
- [29] E. Diaz, A.F. Mohedano, J.A. Casas, L. Calvo, M.A. Gilarranz, J.J. Rodriguez, *Appl. Catal. B* 106 (2011) 469–475.
- [30] Z.M. de Pedro, E. Diaz, A.F. Mohedano, J.A. Casas, J.J. Rodriguez, *Appl. Catal. B* 103 (2011) 128–135.
- [31] S. Gómez-Quero, F. Cárdenas-Lizana, M.A. Keane, *Chem. Eng. J.* 166 (2011) 1044–1051.